Polarized neutron reflectivity study of spin vortices formed in Gd-based Langmuir-Blodgett films

S. Gayen, M. K. Sanyal, and A. Sarma
Surface Physics Division, Saha Institute of Nuclear Physics, 1/AF Bidhannagar, Kolkata 700064, India

M. Wolff, K. Zhernenkov, and H. Zabel
Lehrstuhl für Festkörperphysik/Experimentalphysik, Ruhr-Universität Bochum, 44780 Bochum, Germany
(Received 9 July 2010; revised manuscript received 21 July 2010; published 22 November 2010)

Results are reported of a polarized neutron reflectivity (PNR) study of Gd-based Langmuir-Blodgett films in the temperature range of 55 mK to 15 K, representing two-dimensional magnets. A model based on in-plane spin vortices can explain the low-field as well as high-field PNR data. The branching of zero-field-cooled and field-cooled magnetization curves are explained by reconfiguration of the vortex structure. The low-field magnetization data is found to follow a power-law behavior as predicted by the Berezinskii-Kosterlitz-Thouless (BKT) transition for a finite-size system. We have also observed that a field of 15 kOe annihilates vortex-antivortex pairs completely to produce a homogeneous phase with saturation moment $\sim 7\ \mu_B$ per Gd ion below the BKT transition temperature ($\simeq 600$ mK).

DOI: 10.1103/PhysRevB.82.174429 PACS number(s): 75.70.Ak, 75.25.−j, 75.50.Xx

I. INTRODUCTION

Spin vortices are most appealing characteristics of two-dimensional (2D) easy-plane spin systems which are receiving recent attention[1,2] for their fundamental properties and possible technological applications involving nanostructured magnetic materials. Spin vortices are in-plane circular spin arrangements which may have core spins directing out-of-plane to reduce exchange energy.[2] A spin vortex exists together with its counterpart, known as anti-vortex, as a pair below a characteristic temperature, T_{BKT}, defined by scaling of spin-spin correlation and susceptibility.[3] The unbinding of vortex pairs above T_{BKT} is known as the Berezinskii-Kosterlitz-Thouless (BKT) transition.[4] A sufficiently strong in-plane magnetic field, below T_{BKT}, may cause the core of a vortex to move toward the core of an antivortex so that the cross-tie domain walls become annihilated, resulting in a homogeneous magnetization.[1] Above T_{BKT}, the vortices are free and may also be generated but no field can annihilate such individual topological defects.[1] Hence the saturation moment above T_{BKT} along an applied field is expected to saturate at much lower values than that obtained in a homogeneous phase. These characteristics are opposite to what one expects for systems having a canted phase, a metamagnetic phase or a blocking behavior, where elevated temperature helps to reach a higher saturation moment along any field direction. For a real 2D system, a measurable finite-size-induced spontaneous magnetization below T_{BKT} follows a power-law scaling for BKT transition: $M \sim (T_{\mathrm{BKT}} - T)^{\beta}$, where $\beta = 3\pi^2/128 = 0.231$.[5]

Here, we show that polarized neutron reflectivity (PNR),[6] a nondestructive technique, can be employed to investigate the spin reconfiguration of in-plane vortex structures as a function of applied magnetic field and temperature. The magnetic force microscopy[2] probes the local out-of-plane spin structures at the center of each vortex while PNR can provide direct information about in-plane spin arrangements averaged over the coherence volume of the neutron beam. The PNR techniques could be successfully used to study noncollinear spin arrangements such as canted phases[7] and chiral spin structures of exchange springs,[8,9] and also to study the vortices in thin-film superconductors.[10] Simultaneous measurements of the in-plane magnetization components parallel and perpendicular to the applied magnetic field[11] has made PNR a unique technique to study in-plane spin vortices. Moreover, associated nuclear scattering provides a calibration of the average magnetic moment per scatterer in the units of Bohr magneton (μ_B).

We could investigate in-plane vortices at sub-Kelvin temperature using PNR due to the presence of a large number of noninteracting stacks of Gd monolayers (refer to the schematic in Fig. 1) each forming a 2D magnet in Gadolinium-stearate (GdSt) Langmuir-Blodgett (LB) films.[12] Earlier studies[12] showed that these films exhibit (a) paramagnetism when data are collected by applying a field normal to the film surface; (b) a saturation in magnetization with an applied in-plane field indicating $J_z \approx 0$ and $J_{xy} \neq 0$; and (c) the value of in-plane saturation moment was found to increase exponentially with lowering of temperature showing a constant value below 500 mK. Much lower value of 5.4 μ_B than the expected saturation moment of $\sim 7\ \mu_B$ per Gd ion, even in presence of 40 kOe field, was interpreted as existence of a heterogeneous phase and the exponential decay of the saturation moment at higher temperature was assumed to be due to a reduction in the correlation length. But the earlier pro-

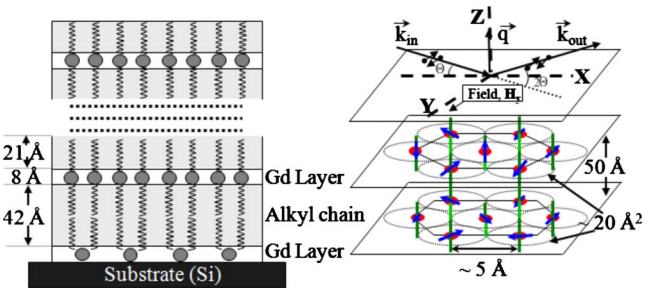

FIG. 1. (Color online) Schematic structure of GdSt multilayer LB film: out-of-plane stacking and layered arrangement of in-plane spins with specular reflectivity geometry.

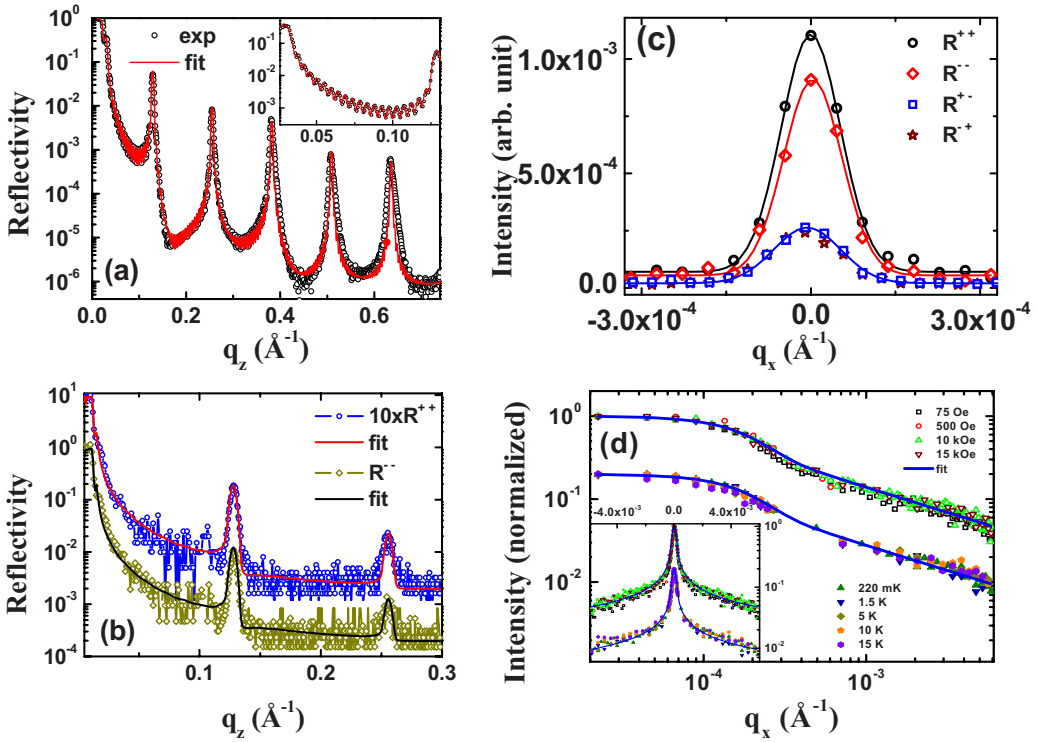

FIG. 2. (Color online) (a) Specular x-ray reflectivity of GdSt LB film with 25 monolayers, showing distinct Bragg peaks and Kiessig fringes (inset). Open circles are experimental data points and solid line is the fitted curve. (b) PNR data and fitted curve with distinct NSF Bragg peaks collected at 220 mK with 1 kOe in-plane field. For clarity R^{++} data is shifted by one decade. (c) Typical rocking curve at the first Bragg peak with 75 Oe field (NSF and SF) during ZFC measurement at 130 mK. (d) Off-specular diffuse intensity (R^{++}, normalized) at 220 mK for different in-plane fields (upper one) and at different temperature with 15 kOe field (lower one, divided by five). The log-linear plot is in the inset. The solid line is a fit with a Kummer function.

posed model[12] could not explain branching of the zero-field-cooled (ZFC) and field-cooled (FC) magnetization data taken with 100 Oe in-plane field. Moreover, our present PNR study at milli-Kelvin temperature with an accurate calibration of the average Gd moment confirms the presence of a homogeneous (in-plane) magnetic phase giving $\sim 7\ \mu_B$ per Gd ion[13] below 500 mK. The lower saturation moment of 5.4 μ_B obtained in the dc magnetization measurement is due to overestimation of Gd-covered area of the film. The results of our present neutron diffuse scattering study also show that the in-plane correlation length does not increase as the temperature becomes lower. We show here that all experimental observations can be explained using a model based on a cross-tie configuration of a vortex-antivortex annihilation process predicted through micromagnetic simulations[1] with $T_{\mathrm{BKT}} \simeq 600$ mK. Such a low value of T_{BKT} is expected here due to the presence of spin vacancies[14] arising due to pin holes.[15]

II. EXPERIMENTAL DETAIL

The experiments were performed on GdSt LB films, consisting of 51 monolayers (101 dippings). The films were deposited using conventional LB technique by transferring GdSt, formed at the water-air interface to a previously hydrophilized (according to Radio Corporation of America (RCA) cleaning procedure with ammonium hydroxide and hydrogen peroxide solutions) silicon substrate (2×2 cm^2) using an alternating trough (KSV 5000). The details of deposition and characterization have been reported earlier.[12]

The specular reflectivity with the momentum transfer $q_z = (4\pi/\lambda)\sin\theta$, where θ denotes the angle of incidence (and reflection), provides electron/scattering-length density averaged across the coherence volume of the x-ray/neutron beam in the plane of the sample surface (xy plane) as a function of depth (z).[15,16] A typical x-ray reflectivity scan is shown in Fig. 2(a) with a simple model fit [16] for a film having 25 monolayers. The in-plane structure is hexagonal with a Gd-Gd separation of 5 Å and with an in-plane correlation length of 100–150 Å.[17] The PNR measurements were carried out with an angle dispersive neutron reflectometer ADAM (Ref. 18) at the Institut Laue Langevin (Grenoble, France) using a monochromatic beam of wavelength, $\lambda = 4.41$ Å. The sample was mounted vertically on a copper plate and was placed in a helium cryostat with vertical magnetic field option. The ZFC-FC data were taken during warming after cooling the sample from 1.2 K to the base temperature 55 mK in the absence (ZFC) or presence (FC) of a small in-plane field.

Neutrons arriving at the sample surface are spin polarized either parallel (+) or antiparallel (−) to the magnetic field H applied along the y direction (refer to Fig. 1). The reflected neutrons carry information regarding the refractive index, $n^{\pm}(z)$ of the medium. The refractive index profile represents nuclear and magnetic scattering contributions that can be expressed as

$$n^{\pm}(z) = 1 - \frac{\lambda^2}{2\pi}\left(\frac{b}{v} \mp c\mu\right), \quad (1)$$

where b/v is the complex nuclear scattering amplitude per unit volume and $c = m_n\mu_n/2\pi\hbar^2$ $(=2.3\times10^{-10}$ Å^{-2} Oe$^{-1})$ and $\mu(\mu_x, \mu_y, \mu_z)$ is the magnetization. The polarization of the reflected beam was measured to obtain four different cross sections designated as R^{++}, R^{--}, R^{+-}, and R^{-+} where the superscripts indicate the polarization of incident and reflected neutron beam, respectively. Typical nonspin-flip (NSF) data, R^{++} and R^{--}, with fitted curves[16] are shown in Fig. 2(b). The difference of NSF intensity, as evident in the rocking curves shown Fig. 2(c) around the first Bragg peak gives the magnetization parallel to the applied field $[(R^{++}-R^{--}) \propto \langle\mu_y\rangle]$. The obtained values for $\langle\mu_y\rangle$ are calibrated in μ_B units as we fit both R^{++} and R^{--} reflectivity data simultaneously using Eq. (1). The SF intensities, R^{+-} and R^{-+} reflectivities are purely of magnetic origin and depend on the average square of the transverse in-plane magnetic moment, $\langle\mu_x^2\rangle$.[11] The PNR data, collected in this geometry, are insensitive to the out-of-plane moment μ_z.

III. RESULTS AND DISCUSSION

It is to be noted here that for a perfect vortex (or antivortex) existing within the coherence volume of the neutron beam, $\langle\mu_y\rangle$ $(\equiv\langle\mu_x\rangle)$ will be zero whereas $\langle\mu_x^2\rangle$ will be finite. Same result is expected for conformal multilayered films where the vertical correlation length extends beyond the coherence volume of the neutron beam. Measured values of $\langle\mu_x^2\rangle$ and $\langle\mu_y\rangle$ by PNR data are expected to deviate from this ideal condition as a real multilayered film is not perfectly conformal and the data are collected in presence of an applied field. Nevertheless the measured value of $\langle\mu_x^2\rangle$ is expected to decrease continuously with corresponding increase in $\langle\mu_y\rangle$ as the applied field is increased.

The presence of central peaks in the diffuse scattering data collected along the q_x direction for both NSF and SF data clearly indicates that the interfaces are correlated.[15] The diffuse data in the NSF channel was found to be independent of applied field and temperature [refer peak-normalized representative data in Fig. 2(d)]. The diffuse scattering profile $I(q_x)$ as a function of the in-plane momentum transfer, q_x $[=2\pi(\cos\theta_i - \cos\theta_f)/\lambda$ with θ_i and θ_f as incident and outgoing angles, respectively] at the first Bragg peak $(q_z=0.128$ Å$^{-1})$ for the NSF data have been analyzed using the hypergeometric Kummer function[19]

$$I(q_x, q_z) = R(q_z)\,{}_1F_1\left(\frac{1-\eta}{2}; \frac{1}{2}; \frac{-q_x^2\zeta^2}{4\pi^2}\right), \quad (2)$$

where $R(q_z)$ is the NSF reflectivity (R^{++} and R^{--}) at $q_x=0$. The Kummer function provides Gaussian-type profile for the resolution function and $\zeta=10.5$ μm is the neutron coherence length. The diffuse tail having a constant slope in log-log plot [refer to Fig. 2(d)] also comes out from the Kummer function and the exponent $\eta=\frac{1}{2}Bq_z^2$ dictates the peak-to-diffuse-tail ratio. We obtained $B=49.43\pm4.0$ Å^2 from these neutron data whereas for a similar LB film a B value of 2.1 Å^2 was found by x-ray scattering.[19] The higher scattering density contrast in neutron scattering between organic "tail" and "head" (Gd-COO$^-$) parts of each GdSt layer provides a better measure of fluctuations. The higher value of B obtained here signifies larger conformal fluctuations from the average position of the interfaces. The peak-to-tail ratio for SF data was found to be lower than that of NSF data [refer to Fig. 2(c)] due to a higher peak width signifying that the magnetic correlation length is shorter than the structural correlation length. We could not quantify this result as SF intensity could not be measured over a large q_x range due to weak intensity but the width of the SF peak was found to be independent of temperature. The conformality of vortex structure can happen due to an alignment of vortex cores across the interfaces around pin-hole defects.[15]

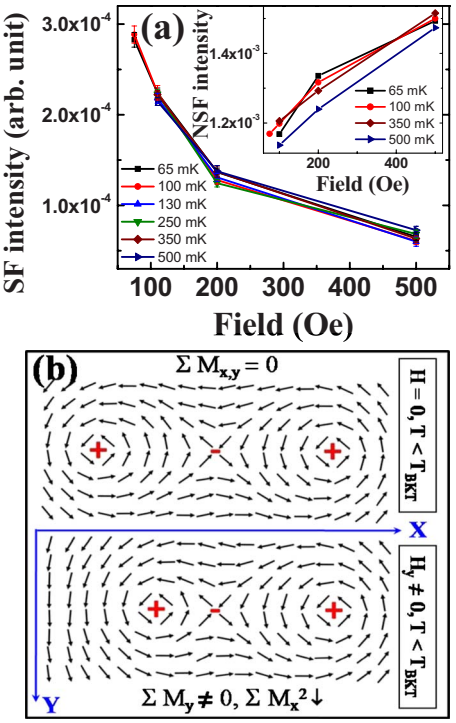

FIG. 3. (Color online) (a) Variation in SF and NSF (inset) intensity from ZFC state at the first Bragg peak with fields. (b) Schematic of in-plane spin configuration in bound vortex $(\oplus)$ and antivortex $(\ominus)$ state below T_{BKT} in absence and presence of an in-plane field along the direction perpendicular to the cross-tie wall (y direction).

The SF intensity [refer to Fig. 3(a)] at various temperatures was observed to decrease with increasing applied field, H_y. The decrease in intensity $(\sim2.3\times10^{-4})$ in the SF channel (R^{+-}) for variation in applied field from 75 to 500 Oe is about the same as the increase in R^{++} [inset Fig. 3(a)] for the same variation in field. The systematic drop of SF intensity with stronger fields is consistent with vortex reconfiguration. It was also observed that for a 100 Oe field the SF intensity in the FC phase was lower in value $(\sim2.12\times10^{-4})$ than the corresponding value $(\sim2.26\times10^{-4})$ in the ZFC phase which is expected for a vortex state. It is known from micromagnetic simulations[1] that the increase in H_y causes a vortex core $(\oplus)$ to move closer to an antivortex core $(\ominus)$, resulting in an

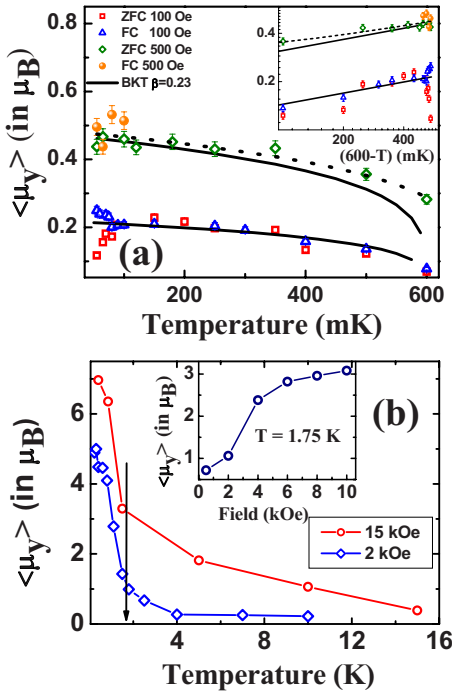

FIG. 4. (Color online) (a) Low-field ZFC-FC magnetization (in Bohr magneton) curves for 100 and 500 Oe applied in-plane field with a power law fit (solid and dashed lines) following BKT transition (log-log plot in the inset). (b) High-field Magnetization curves for 15 and 2 kOe fields.

increase in $\langle \mu_y \rangle$ [refer to Fig. 3(b)] and corresponding decrease in transverse component ($\langle \mu_x^2 \rangle$). The SF intensities for different fields were found to be almost independent of temperature below 600 mK.

A branching in the ZFC-FC magnetization, $\langle \mu_y \rangle$, showing lower value in ZFC [refer to Fig. 4(a)] was obtained, as earlier[12] around 100 mK with 100 Oe in-plane field. The corresponding SF intensity in the ZFC state was found to be higher than the FC state. The maximum in-plane moments $\langle \mu_y \rangle$, measured at 100 mK with 100 Oe and 500 Oe are only around 3% and 7% of the saturation value of 7 μ_B, respectively. Such small values of in-plane magnetization are not due to an antiferromagnetic spin arrangement which would give rise to additional half-order peaks in reflectivity data.[20] The continuous rise of the average in-plane moment, $\langle \mu_y \rangle$ along the field direction with increasing temperature up to 100 mK for the ZFC curve with 100 Oe field cannot be explained as a typical blocking phenomena. Unusual low branching temperature, $T_B \simeq 100$ mK ($\equiv 8.3$ μeV/k_B) observed here is energetically equivalent to a field of 1.43 kOe ($\equiv 8.3$ μeV/μ_B), indicating that the absence of branching with a field of 500 Oe is not simply like overcoming the anisotropy barrier that causes blocking or canting.[21] The observed ZFC-FC branching here can be explained by assuming that the spin configurations shown schematically in the upper and lower panels in Fig. 3(b) represent the ZFC and FC state, respectively. At a temperature below T_B, the measured $\langle \mu_y \rangle$ in a field will be lower in the ZFC state than that of the FC state as the upper spin configuration of Fig. 3(b) cannot become the same as the lower one due to associated topological rigidity. Above T_B, these two configurations become indistinguishable and it is expected that in higher fields, T_B will be lower. The temperature dependence of the low field (100 Oe) magnetization, $\langle \mu_y \rangle$ fits well with the power-law scaling of magnetization with β=0.23 for the BKT transition temperature, T_{BKT}=600 mK. For the same value of β we find a deviation for the 500 Oe field data and a better fit (the dashed line) requires the T_{BKT} to be 670 mK. It is expected that T_{BKT} may effectively increase in the presence of a weak in-plane magnetic field that binds some vortex pairs more tightly to exist even at $T > T_{BKT}$.[22]

The characteristics of 2D easy-plane systems having a vortex state is expected to be completely different above and below T_{BKT} ($\simeq$600 mK here). Below T_{BKT} these systems can become homogeneous through annihilation of all vortex-antivortex pairs provided the applied in-plane field is strong enough to align all spins parallel to the field direction giving full saturation moment. At 220 mK with a field of H_y=15 kOe, the magnetization, $\langle \mu_y \rangle$, extracted from PNR, was indeed observed to saturate at 6.96 μ_B with an error bar of $\pm 5\%$ [refer to Fig. 4(b)]. However, for lower applied field below T_{BKT} the core of vortices may survive and the saturation moment will be lower than the full value. For example, with 2 kOe applied field we get a saturation value of 5 μ_B [refer to Fig. 4(b)]. It is known from theory of vortex states that for $T > T_{BKT}$ free vortices not only exist but may also be generated and cannot be annihilated individually[1]—this hinders the process of having a saturation with full moment even in very high applied field. The inset of Fig. 4(b) shows a typical example: with 10 kOe field at 1.75 K the apparent saturation moment is 3.6 μ_B. The vortex model, presented here, also explains the earlier results obtained with these films showing a continuous reduction in the saturation moment with increasing temperature even in strong in-plane magnetic fields.[12]

In conclusion, extensive neutron reflectivity results presented here are consistent with the presence of spin vortices in monolayers of Gd ions. Measured average saturation moments above and below the transition temperature ($T_{BKT} \simeq 600$ mK) could be explained by unbound and bound vortex structures, respectively.

ACKNOWLEDGMENTS

S.G. and M.K.S. acknowledge the financial support of Department of Science and Technology, India for carrying out the experiment at the Institut Laue Langevin, Grenoble, France. M.W., K.Z., and H.Z. acknowledge BMBF funding under Grant No. 05KN7PC1.

[1] T. Okuno, K. Mibu, and T. Shinjo, J. Appl. Phys. **95**, 3612 (2004); K.-S. Lee, B.-W. Kang, Y.-S. Yu, and S.-K. Kim, Appl. Phys. Lett. **85**, 1568 (2004); R. Hertel and C. M. Schneider, Phys. Rev. Lett. **97**, 177202 (2006).

[2] M. Hehn, K. Ounadjela, J.-P. Bucher, F. Rousseaux, D. Decanini, B. Bartenlian, and C. Chappert, Science **272**, 1782 (1996); T. Shinjo, T. Okuno, R. Hassdorf, K. Shigeto, and T. Ono, *ibid.* **289**, 930 (2000); J. Miltat and A. Thiaville, *ibid.* **298**, 555 (2002).

[3] D. G. Wiesler, H. Zabel, and S. M. Shapiro, Z. Phys. B: Condens. Matter **93**, 277 (1994).

[4] V. L. Berezinskii, Zh. Eksp. Teor. Fiz. **59**, 907 (1970) [Sov. Phys. JETP **32**, 493 (1971)]; J. M. Kosterlitz and D. J. Thouless, J. Phys. C **6**, 1181 (1973).

[5] S. T. Bramwell and P. C. W. Holdsworth, J. Phys.: Condens. Matter **5**, L53 (1993); F. G. Mertens, A. R. Bishop, G. M. Wysin, and C. Kawabata, Phys. Rev. Lett. **59**, 117 (1987); S. T. Bramwell and P. C. W. Holdsworth, Phys. Rev. B **49**, 8811 (1994).

[6] O. Halpern and M. H. Johnson, Phys. Rev. **55**, 898 (1939); R. M. Moon, T. Riste, and W. C. Koehler, *ibid.* **181**, 920 (1969); C. F. Majkrzak, Physica B **173**, 75 (1991); S. J. Blundell and J. A. C. Bland, Phys. Rev. B **46**, 3391 (1992); G. P. Felcher, Physica B **192**, 137 (1993).

[7] B. C. Choi, A. Samad, C. A. F. Vaz, J. A. C. Bland, S. Langridge, and J. Penfold, Appl. Phys. Lett. **77**, 892 (2000); S. Roy, M. R. Fitzsimmons, S. Park, M. Dorn, O. Petracic, I. V. Roshchin, Z.-P. Li, X. Batlle, R. Morales, A. Misra, X. Zhang, K. Chesnel, J. B. Kortright, S. K. Sinha, and I. K. Schuller, Phys. Rev. Lett. **95**, 047201 (2005).

[8] K. V. O'Donovan, J. A. Borchers, C. F. Majkrzak, O. Hellwig, and E. E. Fullerton, Phys. Rev. Lett. **88**, 067201 (2002).

[9] M. R. Fitzsimmons, S. D. Bader, J. A. Borchers, G. P. Felcher, J. K. Furdyna, A. Hoffmann, J. B. Kortright, I. K. Schuller, T. C. Schulthess, S. K. Sinha, M. F. Toney, D. Weller, and S. Wolf, J. Magn. Magn. Mater. **271**, 103 (2004).

[10] S.-W. Han, J. F. Ankner, H. Kaiser, P. F. Miceli, E. Paraoanu, and L. H. Greene, Phys. Rev. B **59**, 14692 (1999); S.-W. Han, J. Farmer, H. Kaiser, P. F. Miceli, I. V. Roshchin, and L. H. Greene, *ibid.* **62**, 9784 (2000).

[11] H. Zabel and K. Theis-Bröhl, J. Phys.: Condens. Matter **15**, S505 (2003); H. Zabel, K. Theis-Bröhl, and B. P. Toperverg, in *The Handbook of Magnetism and Advanced Magnetic Materials: Novel Techniques*, edited by H. Kronmller and S. P. S. Parkin (Wiley, New York, 2007), Vol. 3, pp. 2327–2362.

[12] M. K. Mukhopadhyay, M. K. Sanyal, M. D. Mukadam, S. M. Yusuf, and J. K. Basu, Phys. Rev. B **68**, 174427 (2003); M. K. Mukhopadhyay, M. K. Sanyal, T. Sakakibara, V. Leiner, R. M. Dalgliesh, and S. Langridge, *ibid.* **74**, 014402 (2006).

[13] L. T. Baczewski, P. Pankowski, A. Wawro, K. Mergia, S. Messoloras, and F. Ott, Phys. Rev. B **74**, 075417 (2006).

[14] S. A. Leonel, P. Zimmermann Coura, A. R. Pereira, L. A. S. Mól, and B. V. Costa, Phys. Rev. B **67**, 104426 (2003).

[15] J. K. Basu and M. K. Sanyal, Phys. Rep. **363**, 1 (2002).

[16] L. G. Parratt, Phys. Rev. **95**, 359 (1954).

[17] M. K. Mukhopadhyay, M. K. Sanyal, A. Datta, M. Mukherjee, T. Geue, J. Grenzer, and U. Pietsch, Phys. Rev. B **70**, 245408 (2004).

[18] A. Schreyer, R. Siebrecht, U. Englisch, U. Pietsch, and H. Zabel, Physica B **248**, 349 (1998); M. Wolff, K. Zhernenkov, and H. Zabel, Thin Solid Films **515**, 5712 (2007).

[19] M. K. Sanyal, S. K. Sinha, K. G. Huang, and B. M. Ocko, Phys. Rev. Lett. **66**, 628 (1991); J. K. Basu, S. Hazra, and M. K. Sanyal, *ibid.* **82**, 4675 (1999).

[20] V. Leiner, K. Westerholt, A. M. Blixt, H. Zabel, and B. Hjörvarsson, Phys. Rev. Lett. **91**, 037202 (2003); J. Meersschaut, C. Labbe, F. M. Almeida, J. S. Jiang, J. Pearson, U. Welp, M. Gierlings, H. Maletta, and S. D. Bader, Phys. Rev. B **73**, 144428 (2006).

[21] Spin canting (Refs. 7–9) is not expected in our GdSt films as orbital moment is quenched (7 μ_B comes from Gd^{+3} valence state).

[22] M. E. Gouvêa, F. G. Mertens, A. R. Bishop, and G. M. Wysin, J. Phys.: Condens. Matter **2**, 1853 (1990).